

1 **Ribosome-linked mRNA-rRNA chimeras reveal active novel virus host associations.**

2 **Authors:** J. Cesar Ignacio-Espinoza<sup>1</sup>, Sarah M. Laperriere<sup>1</sup>, Yi-Chun Yeh<sup>1</sup>, Jake Weissman<sup>1</sup>, Shengwei Hou<sup>1</sup>, Andrew  
3 M. Long<sup>\*1</sup>, & Jed A. Fuhrman<sup>1</sup>

4

5 Affiliations:

6 1. Department of Biological Sciences, University of Southern California, Los Angeles CA 90089.

7 ♣ Current address: Department of Oceanography and Coastal Sciences, Louisiana State University, Baton Rouge, LA 70803

8

9 Correspondence to be addressed to: [j.cesar.ignacio@gmail.com](mailto:j.cesar.ignacio@gmail.com) & [fuhrman@usc.edu](mailto:fuhrman@usc.edu)

10

11 **Abstract**

12 Viruses of prokaryotes greatly outnumber their hosts<sup>1</sup> and impact microbial processes across  
13 scales, including community assembly, evolution, and metabolism<sup>1</sup>. Metagenomic discovery of  
14 novel viruses has greatly expanded viral sequence databases, but only rarely can viral  
15 sequences be linked to specific hosts. Here, we adapt proximity ligation methods to ligate  
16 ribosomal RNA to transcripts, including viral ones, during translation. We sequenced the  
17 resulting chimeras, directly linking marine viral gene expression to specific hosts by transcript  
18 association with rRNA sequences. With a sample from the San Pedro Ocean Time-series (SPOT),  
19 we found viral-host links to Cyanobacteria, SAR11, SAR116, SAR86, OM75, and  
20 Rhodobacteraceae hosts, some being the first viruses reported for these groups. We used the  
21 SPOT viral and cellular DNA database to track abundances of multiple virus-host pairs monthly  
22 over 5 years, e.g. with *Roseovarius* phages tracking the host. Because the vast majority of  
23 proximity ligations should occur between an organism's ribosomes and its own transcripts, we  
24 validated our method by looking for self- vs non-self mRNA-rRNA chimeras, by read recruitment  
25 to marine single amplified genomes; verifiable non-self chimeras, suggesting off-target linkages,  
26 were very rare, indicating host-virus hits were very unlikely to occur by mistake. This approach  
27 in practice could link any transcript and its associated processes to specific microorganisms.

28

29 **Main**

30 Microbial communities are central players in the elemental transformations that sustain life on  
31 our planet<sup>2</sup>. Like all of life on earth, microbes are susceptible to viral infections, and in the

32 ocean, viruses dominate and exceed their hosts' numbers manifold<sup>1</sup>. While the importance of  
33 virus-host interactions is well recognized, the vast majority viruses observed microscopically  
34 and those discovered in recent years by metagenomic approaches do not have a specifically  
35 known host, so who infects whom remains largely unknown. This problem is nearly axiomatic in  
36 non-marine environments as well, with potential economic, environmental, and health related  
37 impacts. Virus-hosts links are therefore one of the main open questions in environmental  
38 microbiology, and multiple methods have been developed to address this question, ranging  
39 from the informatic (e.g. finding similarities between virus and host genomic sequences<sup>3</sup>) to  
40 recent wet-lab based protocols such as viral tagging<sup>4</sup>, finding viruses in single amplified  
41 genomes<sup>5</sup> or adsorbed to cells<sup>6</sup>, digital PCR<sup>7</sup> and DNA-DNA proximity ligation<sup>8,9</sup>.

42

43 Viruses function and reproduce only when their genes are transcribed and then translated to  
44 proteins by the host's ribosomal machinery. We adapted and applied the well-established  
45 proximity ligation approach<sup>10</sup>, previously used to probe DNA<sup>9</sup>, RNA<sup>11</sup> and Protein<sup>12</sup> interactions,  
46 to bond the viral transcripts to the host's ribosomal RNA after chemically fixing them both in  
47 the act of translation, thus allowing us to associate viral gene transcripts directly to the host  
48 that is translating them. The bioinformatic analysis allowing us to interpret these connections  
49 as virus-host associations is only possible because we now have large libraries of known marine  
50 viral sequences determined metagenomically<sup>13,14</sup> as well as a massive database of ribosomal  
51 RNA sequence from organisms across the entire phylogenetic tree<sup>15</sup>. Chimeric mRNA-rRNA  
52 sequences that have a virus gene fragment next to a host ribosomal RNA sequence fragment  
53 are a "smoking gun" to show an active virus-host link, contrasting with other recent methods  
54 that also report more incidental relationships. Here we present proof of concept and the first  
55 field application of rRNA-mRNA proximity ligation to specifically link viruses and their hosts  
56 through this viral-transcript-host-ribosome connection. We also validate the method by  
57 showing that among rRNA-mRNA chimeras, the vast majority are coded by the same organism's  
58 genome, suggesting false, cross-organism, linkages are exceedingly rare.

59

60 **Summary of Methods**

61 We present XRM-Seq (Ribosome cross-linking and sequencing). Briefly (Figure 1a) described  
62 (See extended methods below): Seawater samples collected in February of 2020 at the San  
63 Pedro Ocean Time series station (SPOT<sup>16</sup>) were filtered serially through an 80  $\mu$ m nylon mesh  
64 and a 1.2  $\mu$ m fiber glass filter to remove most eukaryotes; cells in the filtrate, containing mostly  
65 free-living prokaryotes, were collected on a 0.2  $\mu$ m filter. (1) These cells were fixed with 1%  
66 formaldehyde, cross-linking adjacent proteins to hold ribosomes together. (2) Intact crosslinked  
67 ribosomes and total RNA were extracted using acid phenol-chloroform, particularly from the  
68 interphase<sup>12</sup>, where the protein-RNA complexes migrate. DNA was depleted with two rounds of  
69 DNase treatment. (3) RNA was randomly cut with micrococcal S1 nuclease, cleaving accessible  
70 rRNA strands in the ribosome (Suppl. Fig. 1), which is held together by covalent bonds from  
71 crosslinking between the proteins that make most of the ribosomal mass, and it also generates  
72 free ends in the mRNA. (4) Free RNA ends (from ribosomal or messenger RNA) were then  
73 ligated into circular forms with a circRNA ligase<sup>11</sup>. (5) To enrich for chimeric reads, samples  
74 were then subject to degradation of non-circular RNA using RNase R<sup>11</sup>. Crosslinks were cut by  
75 proteinase K. (6) RNA was then retrotranscribed to cDNA, which was then used to prepare  
76 libraries that were then deeply sequenced by Illumina Nova Seq. Merged and QC'ed reads (see  
77 extended methods below) were then searched for chimeric reads by aligning them against Silva  
78 v 132<sup>15</sup>, single cell genomes<sup>17</sup>, a local rRNA sequence database<sup>18</sup>, a set of local viral contigs  
79 (representing 5 years of monthly samples) from our previous metagenomic work<sup>13</sup> and our in-  
80 house database of fully sequenced marine viruses, fosmids and assemblies from global marine  
81 virus metagenomics projects.

82

### 83 **Results and Discussion**

84 *We validated our method and found a negligible rate of false positive linkages.* The general  
85 validity of the approach was verified by examining chimeric linkages for those between rRNA  
86 and protein-coding genes from the same organisms, which would be expected to be the vast  
87 majority of linkages if the method worked as planned. For this validation we wanted to use  
88 independently-determined and bona fide genome sequences, so we did not try to bin genomes  
89 from our own local metagenomic data (to avoid assembly artifacts or any possible circular

90 reasoning), but instead used published marine genomes as a reference set. In particular, we  
91 used sequences from a recently released set of tropical and subtropical marine single amplified  
92 genomes (SAGs)<sup>17</sup>. This analysis showed that the vast majority these linkages were to the same  
93 SAG or within the same close lineage (Figure 1b); Because these SAGs were not from our exact  
94 site, we expect that these close (but not perfect) hits are due to database imperfections (i.e.  
95 our local organism may not match a SAG exactly but may have two similarly-close SAG relatives)  
96 and not because erroneous, i.e. non-self, linkages somehow always happened to occur only  
97 with close relatives. Erroneous linkages would instead be expected to occur randomly among  
98 and across the several most abundant and diverse taxa, which was not observed. Thus these  
99 results validate our approach, and we felt confident extending the analyses to virus-host  
100 linkages

101

102 *mRNA-rRNA chimeras reveal novel virus-host links.* To cast the widest possible net for potential  
103 viruses and hosts in the chimeric linkages, we took advantage of the fact that we have been  
104 studying the SPOT site for several years, and have considerable existing metagenomic (from  
105 viruses) as well as rRNA sequence data. We used these local databases, including all contigs  
106 from our previously published 5-year viral metagenomic dataset<sup>13</sup>, SILVA v. 132<sup>15</sup> and our  
107 collection of rRNA clones collected as part of our long-term SPOT ecological time series<sup>16</sup>. We  
108 updated the characterization of viral contigs in our 0.02-0.2  $\mu$ m size fraction viral metagenome,  
109 by adding newer and more sensitive virus-finding tools to the previous application of VirSorter  
110 and VirFinder (confirmatory), specifically DeepVirFinder, CheckV, MEGAN-LR, VirSorter, and  
111 homologies to the Tara Ocean proteomic datasets (see methods). We then mapped reads with  
112 an overlap > 100 bp and > 95% identity to all the assembly from San Pedro Virome dataset,  
113 Searching for rRNA ligated to newly identified viral contigs, we identified 699 mRNA-rRNA  
114 chimeric reads, which represented 46 different viral contigs linked to 16S or 23S rRNA (Figure  
115 2a, Suppl. File 1). We found more associations between mRNA and 16S than 23S rRNA (Fig 2a),  
116 despite 23S being longer, perhaps suggesting 16S has more accessible loops to allow enzymatic  
117 cleavage and re-ligations.

118

119 Our 46 identified viruses include those to hosts for which viruses were previously unknown,  
120 significantly the first SAR86 virus (Figure 2b, Suppl. File 1), particularly notable because this  
121 gammaproteobacterial group is globally abundant in seawater<sup>19</sup>. This virus appears to be an  
122 abundant member of the community at the transcriptomic level, though surprisingly it has no  
123 significant hits in the global ocean virome (GOV) dataset (Figure 2f), suggesting it may be  
124 regional or ephemeral. We also describe the first putative OM75 (alphaproteobacterial) viruses,  
125 and abundant Roseobacter phages unlike those previously reported (Figure 2; Suppl. Table1).  
126 Cyanobacterial viruses were well represented in the host-virus chimeras characterized by our  
127 methods, as expected due to their abundance in our samples, as well as their prevalence in the  
128 cultivated virus database. Phylogenetic 16S assignment divided them between *Prochlorococcus*  
129 (N= 7) and *Synechococcus* (N=3), and one whose associated 16S fragments did not allow us to  
130 distinguish between those two genera (Suppl. File 1; Figure 2b-f). We also found abundant  
131 phages associated with various Alphaproteobacteria, divided among Rhodobacteraceae (N= 132 16), SAR116 (N=8) and phages infecting the abundant SAR11 (N=8). Some of these host  
133 assignments, due to the abundance of the chimeras (many 16S hits), can be placed to the exact  
134 amplicon sequence variant (ASV) level, such as a *Roseovarius*, with multiple viral contig links to  
135 a single 16S ASV (Suppl. Table 1, Figure 3, below), suggesting that they are probably fragments  
136 of the same viral genome.

137  
138 Due to the constraints of the bioinformatic methods used to identified viral contigs (complete  
139 dependencies on databases), it is difficult to identify fully novel viruses, and it is possible that  
140 linkages to many truly novel viruses have been missed by our conservative approach. We  
141 assessed the novelty of the viral lineages linked to particular hosts in our analysis, by identifying  
142 the percentage of known viral genes within a contig (Figure 2e) and the distribution of  
143 nucleotide identities to sequences from GenBank and metagenomic projects (Figure 2f)<sup>14,20</sup>. We  
144 see that most of the contigs have either a good percentage of hits that can be identified as viral  
145 or are represented in public metagenomic projects. Exceptions include the novel SAR86 virus  
146 (mentioned above), an unassigned cyanophage and a phage that we couldn't place to any  
147 phylogenetic group due to the scarcity of the chimeric reads, which appear to be poorly

148 represented in metagenomic assemblies. Beyond absolute novelty, our experiments revealed  
149 viral groups previously reported only to infect very different host groups than we report here,  
150 for example a novel T7-like Roseobacter phage (CT18917, Rank 6, Figure 2) with distant hits to  
151 T7 cyanobacterial phage (Suppl. File 1), and novel SAR11 viruses (CT\_SN\_17500 and  
152 CT\_SN\_38734, Ranks 20 and 21, Figure 2) that appear distantly related to enterobacterial T5  
153 phages. This expands the range of known viruses infecting this numerically dominant ocean  
154 clade.

155

156 We can track viruses and their presumed host abundances from our San Pedro Time series, and  
157 interestingly we find contrasting virus-host patterns. The tracking is possible because we used  
158 the assemblies from our recently completed five-year viral metagenomic survey as a database  
159 to find viral sequences, and we can estimate relative abundances via read recruitment to those  
160 data. We also have time series data on potential host relative abundances from amplicon  
161 sequencing of SSU rRNA. Some of the linked viral contigs have many chimeric reads, and this  
162 allowed us to pin-point the specific 16S ASV associated to the host infected by this virus. So we  
163 tracked the long-term (5Yr) virus-host dynamics of these associations (Fig 3). Here we show  
164 three cases, one with a match to a *Synechococcus* ASV, and two with perfect matches a  
165 *Roseovarius* ASV (Suppl. File 1). The abundance of the host ASV in the latter case across time  
166 closely matches the dynamics of the virus in this case (Fig 3), consistent with a persistent virus  
167 infection where the virus essentially tracks the dynamic host abundances over many months.  
168 Yet that is not the only pattern we observed; we also were able to find the specific host for the  
169 third most abundant contig in the 5-year virome, and this cyanophage (Figure 3c-d) and its  
170 associated *Synechococcus* ASV are both dynamic but do not closely track each other. Perhaps  
171 this is due to strain-level variations in viruses and/or hosts that control the extent of infection,  
172 yet variation cannot be detected by short read recruitment nor fairly conserved 16S sequences;  
173 such strain variation is part of the Red Queen-like dynamics we previously reported for this  
174 location<sup>13</sup>. Similar *Synechococcus* strain variation in apparent infection dynamics was also  
175 reported for this location by Ahlgren et al<sup>21</sup>. Note also the cyanophage virus-host pair are both

176 much more abundant than the *Roseovarius* pair, which may also relate to the difference in  
177 patterns.

178

179 We recognize there are potential shortcomings in requiring the virus has a well-assembled  
180 contig in order to match to a host; we know due to high genomic variability, it is often difficult  
181 to assemble many viral contigs in the first place, especially from only one or a few  
182 samples<sup>13,22,23</sup>. So as an alternative approach avoiding the need for assemblies, we searched for  
183 chimeric sequencing reads that aligned to known virus marker genes. We found 171 reads that  
184 match both cyanomyoviral marker gp20 or myoviral marker gp23 as well as a 16S rRNA for host  
185 phylogenetic placement (Figure S2). Not surprisingly, these were enriched for cyanobacterial  
186 viruses (which has a large cultured database) but they also matched, SAR11, SAR92, OM162 and  
187 *Puniceicoccales* (*Verrucomicrobia*), groups for which we have relatively few, if any, previously  
188 known viruses. This shows that our method can operate at the read level, and although the  
189 information is not as satisfactory as having a long viral contig or genome, it is still valuable to  
190 know a particular host is infected by a virus for which we now have at least one specific marker  
191 that can be tracked in metagenomes (for occurrence) or metatranscriptomes (for active  
192 infections) via read recruitment.

193

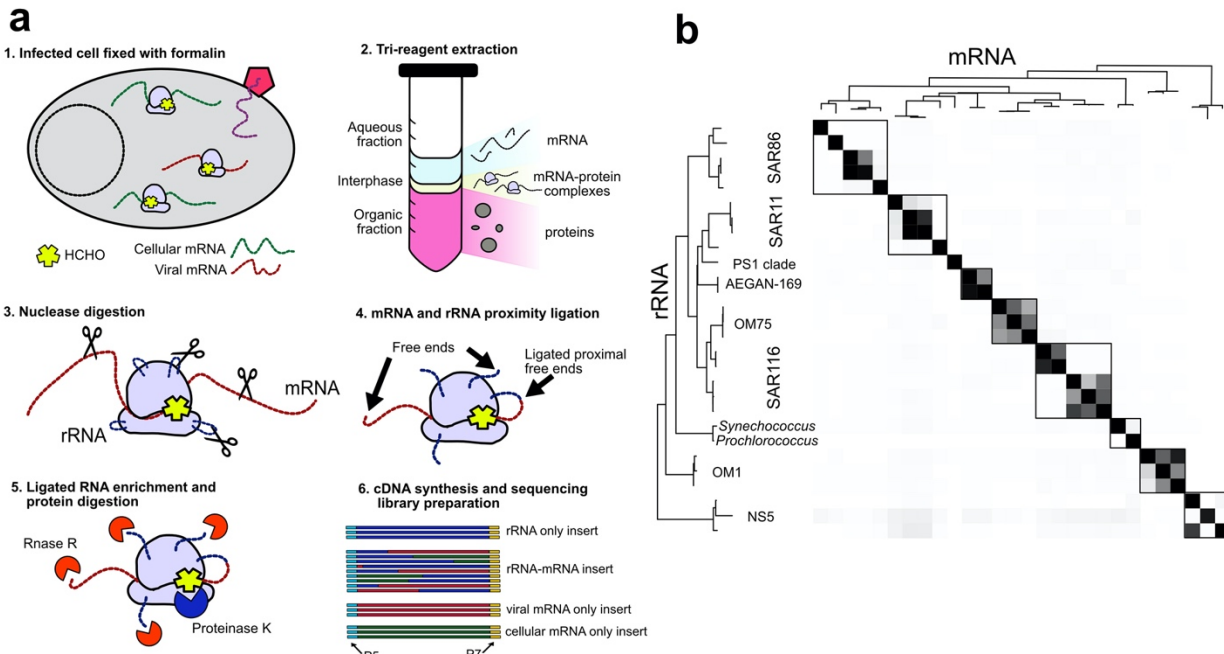
194 In comparison to other methods that aim to link unknown viruses and hosts, this approach has  
195 some obvious advantages. It is much more specific than k-mer baser methods<sup>3</sup>, which are  
196 general purpose and provide probabilities of matches, but typically do not narrow the hosts  
197 down to better than genus or family levels with confidence. It is more high-throughput, and less  
198 costly per match, than methods requiring sequencing sorted cells after amplification<sup>5,6</sup>. It is  
199 most similar to DNA-DNA proximity ligation methods<sup>8,9</sup>, and the principal differences are that  
200 (1) our approach catches the virus in the act of transcription while DNA-DNA approaches will  
201 link any DNA within in close proximity, perhaps catching non-infection situations or  
202 unsuccessful infections, and (2) we can place any host on a phylogenetic tree (or find an exact  
203 match if available) by its 16S (or 23S) rRNA sequence while the general DNA-DNA proximity  
204 ligation method requires host genome sequence information to identify it, and such

205 information on most naturally occurring organisms is limited. One important limitation of our  
206 method is that by the nature of sequencing, the information in short reads is limited. We expect  
207 that future developments such adapting long read sequencing<sup>24</sup> will help overcome this  
208 shortcoming.

209

210 In conclusion, we have adapted molecular biology technique based on proximity ligation and  
211 applied to a first field sample to uncover novel virus-host associations. We anticipate our  
212 methods will be widely applied and improved upon to study the dynamics of interaction  
213 networks in natural environments. Finally, because the proximity ligation is non-specific for  
214 viruses and in fact can associate any translated protein with the ribosome doing the translation,  
215 it can link environmental functions to taxonomic units, much needed for a mechanistic  
216 modeling of a changing ocean.

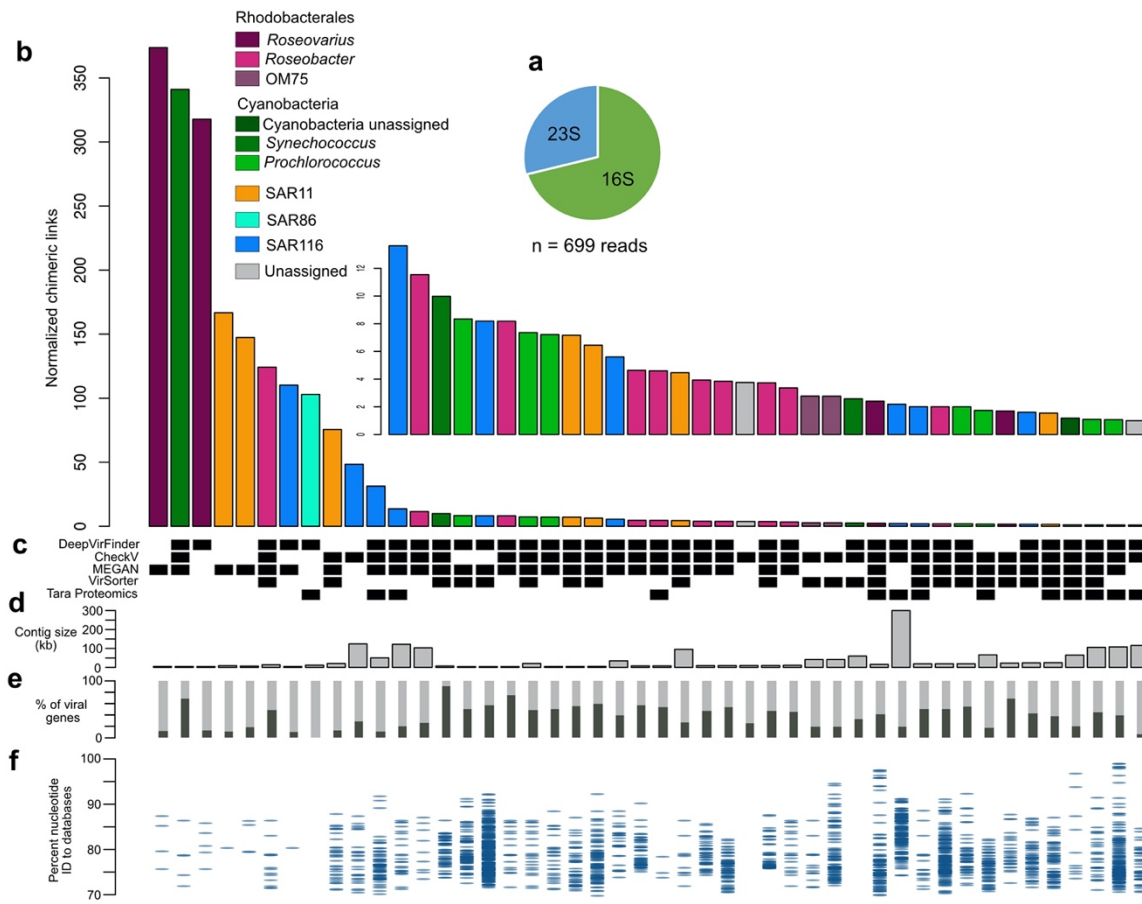
217



218

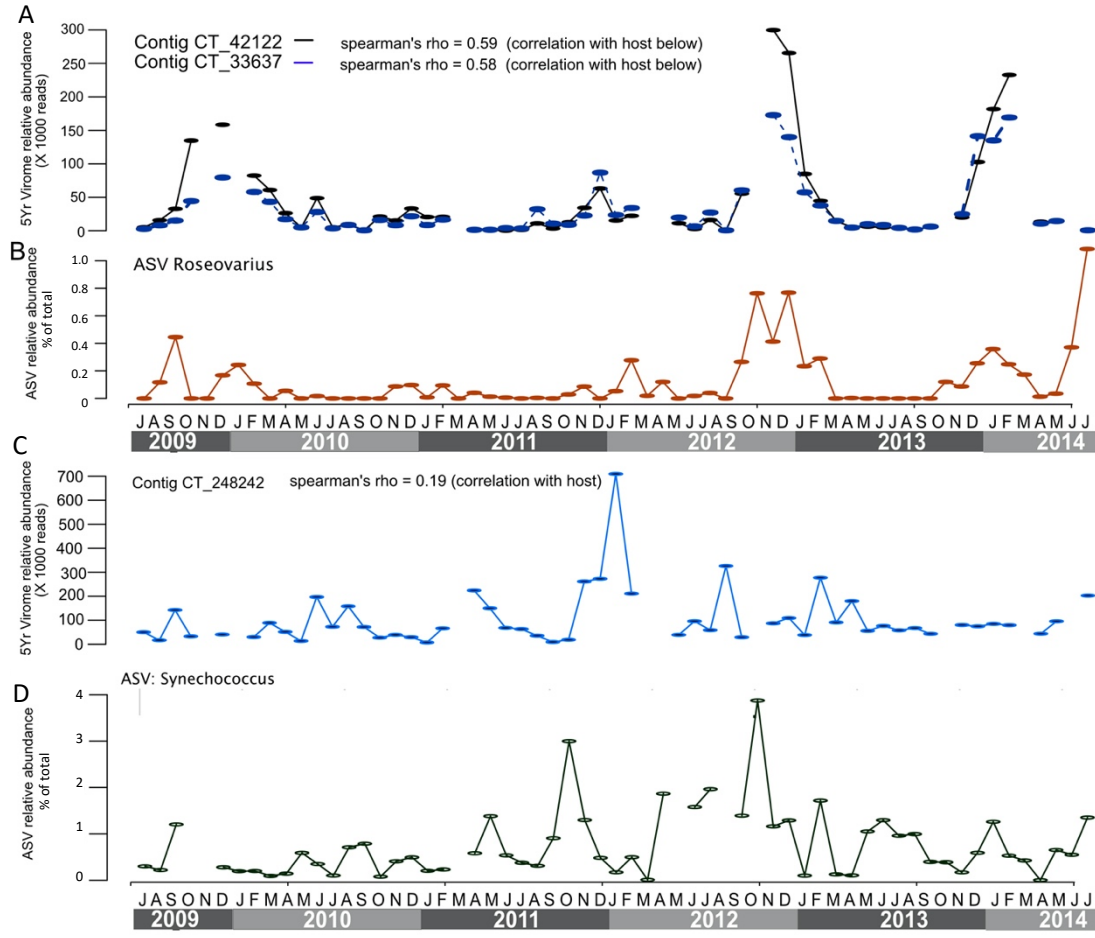
219 **Figure 1.- a)** Diagram of the general method: (1) *In vivo* cross-linking of infected cells in which  
220 formalin fixes ribosome (light purple) complexes during translation of host (green) or virus (red)  
221 mRNA. (2) Acid phenol chloroform extraction separates the components of the cell lysate;  
222 ribosome-mRNA complexes migrate to the interphase. (3) Ribosome complexes are subject to  
223 a nuclease digestion that generates free ends in the rRNA (blue) and mRNA (red). (4) Free  
224 proximal ends are ligated, which generates chimeras. (5) To enrich for ligated RNA, RNA with  
225 exposed ends is degraded with RNase R (orange pie); Crosslinking is reversed with Proteinase K  
226 (dark blue pie). (6) Sequencing libraries were prepared from retrotranscribed purified RNA,  
227 many where chimeric, containing host rRNA (Blue) and viral (red) or host (green) mRNA. **b)**  
228 Validation, based upon mRNA-rRNA chimeras within SAGs, is demonstrated by the strong  
229 domination of within-organism linkages, as expected if the method only links mRNA and rRNA  
230 within each cell, not between cells. This is shown by the taxonomic distribution of chimerically-  
231 linked ribosomal RNA (y-axis) and mRNA transcripts (x-axis), as determined by sequences  
232 mapping to a subtropical-tropical single amplified genome dataset representing all major  
233 marine prokaryotic lineages. Intensity is normalized within rows, reflecting number of linkages,  
234 as determined by sequences mapping (>95 %ID) to a subtropical-tropical single amplified  
235 genome dataset. Tree on left and top (mirrored) is based on 16S rRNA sequences, not similarity  
236 among rows/columns. Note the vast majority of all linkages are either to the identical SAG or to  
237 a very closely related one, the latter probably reflecting situations where our local organism  
238 had no identical SAG but two different very close relatives in the SAG database (accuracy, i.e.  
239 the fraction of self-hits within the shown boxes, is 95%, with an associated *p*-value  
240 <2.2x10<sup>-16</sup>).

241



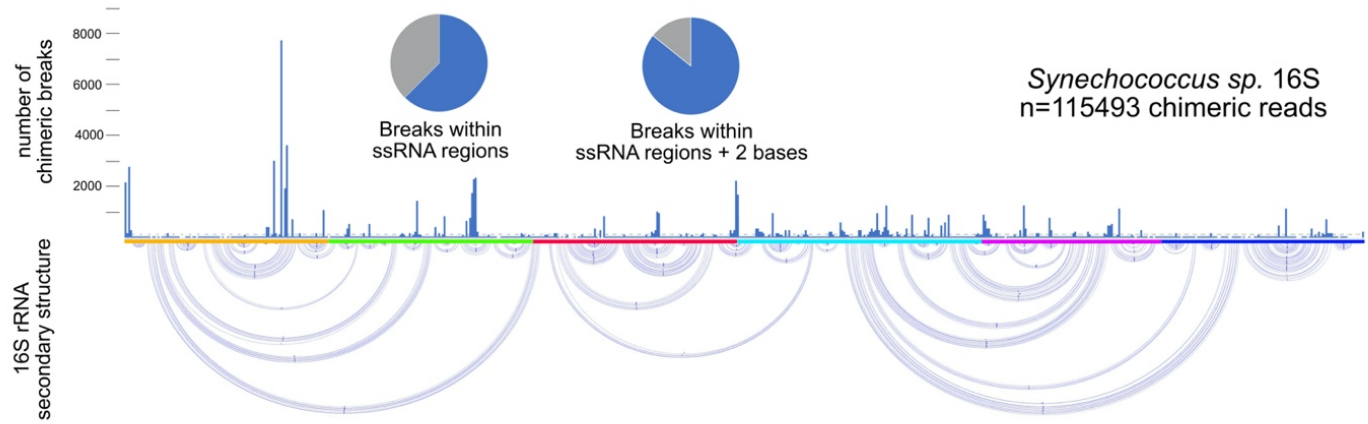
242  
243  
244  
245  
246  
247  
248  
249  
250  
251  
252  
253  
254  
255

**Figure 2.** Novel virus-host associations discovered by RNA proximity ligation. **a)** More rRNA-mRNA chimeras are formed with 16S than 23S rRNA. **b)** Plot of the viral contigs (each bar a different contig) ranked from most to least normalized number of chimeric reads, with colors reflecting the taxonomy of the host from the rRNA within the chimeras. **c)** Black boxes indicating how a contig was identified as viral, methods named on the left. **d)** Length in kb for each contig. **e)** Percentage of genes (dark gray) within each contig currently identified as viral (note uncultivated virus genes are often not known as such) **f)** Distribution of similarity between gene matches obtained from within each contig and genes in public environmental virus databases (GOV and viral isolates from NCBI).



256  
257

258 **Figure 3.** Tracking putative virus-host pairs over five years of ~monthly sampling at the San  
259 Pedro Ocean Time Series. Data are from 16S rRNA amplicons (host ASVs, are shown as  
260 percentage of the total community) and normalized recruitment of 0.02-0.2  $\mu$ m (viral) size  
261 fraction metagenomic reads to viral contigs. **a)** Two virus contigs that both match the same  
262 putative *Roseovarius* host which is shown in **b**. These two contigs are both short (6.1 and 5.4  
263 kbp) and considering the same host match and nearly identical dynamics of both contigs, are  
264 probably from the same virus. Note the general correspondence in abundances over time of  
265 contigs and presumed host, suggesting the virus largely follows its host abundance on this  
266 monthly time scale. **c)** and **d)** show an abundant viral contig and its presumed *Synechococcus*  
267 host, but in this case there is little correspondence between the dynamics, possibly due to  
268 strain variations we cannot detect by 16S and short read recruitment alone.  
269  
270

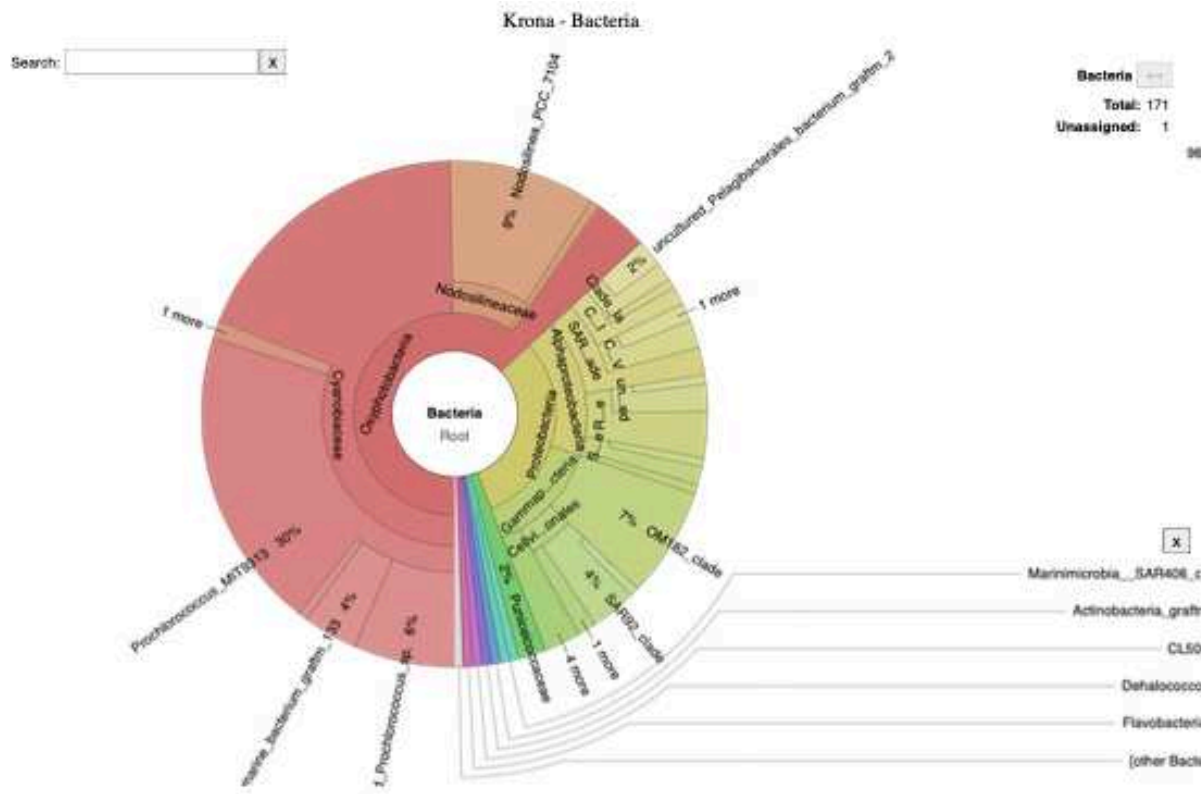


271  
272  
273

274 **Suppl. Figure 1. In accordance with the premise of our experiment the vast majority of the**  
275 **chimeric break points occur in single stranded (loop) regions.** Bottom panel of the figure  
276 represents the known secondary structure of the 16S ribosomal RNA from *Synechococcus*  
277 (<https://crw-site.chemistry.gatech.edu/RNA/Structures/d.16.b.Synechococcus.sp.pdf>). Top  
278 panel shows the number of chimeric read breakpoints at each base, scale on the left side. Pie  
279 charts show the majority of the breaks were at single stranded regions, i.e. loops (or within 2  
280 bases to accommodate natural variation in an environmental sample). Single stranded regions  
281 represent only 1/3 of the length of the 16S rRNA yet it accounts for up to 85% of the  
282 breakpoints; note the breaks are relatively non-random and appear to be enriched at the  
283 beginning of the sequence.

284  
285  
286

287



288

289 **Suppl. Figure 2. Read level analysis reveals potential links between T4-like viral genes and**  
290 **diverse hosts.** We identified reads that matched T4 like genes, and the 16S region of the rRNA-  
291 mRNA chimera was then placed onto a phylogenetic tree using the graftm<sup>25</sup> 16S package. Not  
292 unexpectedly (due to their high representation in the database and also high natural  
293 abundance), cyanobacteria accounted for 60 % of the chimeric reads, but nonetheless T4 is a  
294 widespread family with a great variety of marine hosts.

295 **Materials and Methods:**

296

297         *Sample collection.* Seawater was collected aseptically using a bucket previously stored in  
298 5% HCl during the February 2020 cruise of the San Pedro Ocean Time series  
299 (<https://dornsife.usc.edu/spot/>); 16 L were filtered through a 1 um fiber glass AE filter  
300 (Millipore) to remove larger particles, as well as larger phyto- and bacterioplankton. Filtrate was  
301 then filtered unto a 0.22 um Sterivex cartridge (Millipore, with a Durapore filter); filter was then  
302 dried by pushing air with a 50 mL syringe. We immediately proceeded to crosslink our sample  
303 on this sterivex filter.

304

305         *Crosslinking and RNA extraction.* Samples were fixed with 1% formalin (0.4%  
306 formaldehyde) to create cross-links between adjacent proteins, 2 mL of formalin were added  
307 inside the sterivex cartridges, filter ends covered with locking luer caps, and filter tilted gently  
308 over 5 mins. Excess liquid was pushed out of the sterivex using a clean syringe. Formalin was  
309 then quenched by filling the sterivex cartridge with 250 nM glycine for 20 minutes. Glycine was  
310 pushed out using a clean syringe. Extraction of RNA-Protein complexes was accomplished  
311 largely following the directions described by Trendel et al.<sup>12</sup> modified to accommodate a filter  
312 enclosed in a sterivex cartridge. 1.5 ml of Trizol (Sigma-Aldrich) were added inside the  
313 cartridge, which was capped and mixed for 5 minutes on a vortexer; sterivex cartridge was then  
314 opened again and 0.3 mL of chloroform were added to induce phase separation. The contents  
315 of the sterivex filter (~1.8 mL) were the transferred to a LoBind 2mL tube and rested at room  
316 temperature for 5 minutes. Tubes were centrifuged at 7000 x g and 4C for 10 minutes. RNA was  
317 recovered from the aqueous part following the directions of manufacturer. RNA-Protein  
318 complexes were recovered from the interface as recommended by Trendel et al<sup>12</sup>, resuspended  
319 in 100 uL of DEPC water. RNA from interface and aqueous fraction was then subjected to two  
320 rounds DNase I (NEB) treatment, 100 uL of DNase I (100 Units) and 1.8 mL of 10X DNase buffer  
321 to a final reaction of 2mL. Each time the RNA was concentrated and cleaned by one round of  
322 isopropanol and then one of ethanol precipitation. It was suspended in 100 uL in DPEC water,  
323 quantified with Qbit RNA, we immediately proceeded to the following steps.

324

325         *RNA cleavage and ligation.* RNA was randomly cleaved generating accessible ends both  
326 in the rRNA and mRNA, largely based on the methods by Sharma et al.<sup>11</sup> Multiple 20 uL  
327 reactions were run in parallel, 100 ng of RNA (RNA-protein complexes) each, with 2 Units of S1  
328 enzyme (ThermoFisher, 2 uL of a 1:100 dilution) and 1X S1 Buffer. Reactions were run for 30  
329 mins at room temperature, reactions were stopped by phenol chloroform extraction. Free  
330 mRNA and rRNA ends were then ligated into circular forms with a circRNA ligase (Lucigen); it  
331 favors ligation events between proximal RNA ends<sup>11</sup> and it has limited activity at high  
332 temperature, which would favor ligation of proximal ends only. Specifically, multiple 20 uL  
333 reactions were run in parallel, 50 ng of S1-digested RNA was incubated with 2 uL of 10X circRNA  
334 ligase buffer at 85C for 2 minutes. Tubes were transferred to ice where 1 uL of 10 mM ATP and  
335 1 uL of circRNA ligase were added. Reactions were run at 60C for 60 minutes.

336

337         *Enrichment for Chimeric reads, crosslinking reversal.* Multiple 25 uL reactions were run  
338 in parallel, reactions were set up by adding 0.5 uL of RNaseR (Lucigen), 2.5 uL of RNase R buffer

339 and 2 uL of water to the previous set ups (ligated RNA). These reactions were incubated for 10  
340 minutes at 37C. RNase reactions were stopped with Proteinase K by adding 30 uL of 2X  
341 Proteinase K buffer, 3 uL of Proteinase K and 2 uL of water, reactions were incubated 30  
342 minutes at 60C. Proteinase K treatment also reverses the crosslinking. RNA was purified by  
343 phenol chloroform extraction and suspended in nuclease free water.  
344

345 *Retro transcription and library generation.* Multiple 20 uL reactions were run each with  
346 100 ng of RNA using the NEB first strand synthesis module (Parts no. E7525). 13.5 uL of RNA  
347 and 1 uL of random primers were incubated at 65C for 5 minutes then put on ice. To this, 4 uL  
348 of reaction buffer and 0.5 uL of RNase inhibitor were added, incubated at 25 C for 2 minutes.  
349 Finally 1 uL of Protoscript II reverse transcriptase was added and incubated 10 min at 25 C, 50  
350 at 42C and 15 min at 70C, then put immediately on ice. We then proceeded with the NEB  
351 Second Strand Synthesis Module (Parts no. E7550), by adding 8 uL of the dNTP mix, 4uL of the  
352 enzyme mix and 48 uL of nuclease-free water to a total volume of 80 uL. Reactions were  
353 incubated at 16C for 1 hour. Samples were pooled, cleaned and concentrated using a 1.2 X  
354 AMPure magnetic beads (Beckman-Coulter) and resuspended in 40 uL of low EDTA TE.  
355 Sequencing libraries were generated using the Ovation Ultralow V2 (NuGen) with 14  
356 amplification cycles. Libraries were sent out for sequencing on a 2X250 PE NovaSeq, with a final  
357 sequencing depth of 41 M (aqueous fraction) and 35 M (interface) on each sample. Data from  
358 these two samples was pooled and treated identically in subsequent steps.  
359

## 360 **Bioinformatic analysis.**

361

362 *Quality Control and read merging.* Reads were qc'ed using fastp<sup>26</sup> using a minimum  
363 quality score of 15 covering at least 75 % of the read length (Options: “-q 15 -u 25”) ; we  
364 allowed for a relatively low score value since we use the reads for read recruitment. Reads  
365 were then merged using fastq-join<sup>27</sup> allowing a maximum 10% differences on a minimum 20  
366 bases overlap (Options: “-p 10 -m 20”). In practice this generated an insert size range from 250  
367 bp to 480 bp.  
368

369 *Custom perl scripts:* Custom perl scripts that were written to parse and analyze the data  
370 from our experiment have been deposited at <https://github.com/phagenomics/VirHostLinker>,  
371 they are referenced throughout the methods as <script>.pl <input files>.  
372

373 *A posteriori evaluation of crosslinking specificity.* The initial dataset (76M reads) was  
374 blasted against the collection of single cell genomes from Pachiadaki et al.<sup>17</sup> with all default  
375 options (Options= “blastn -outfmt 6 – num\_threads 8”) , the 16S sequences from these SAGs  
376 were clipped out prior to running the blast program. We then extracted a list of sequences that  
377 matched anything within that database with a percent identity higher than 95% over at least  
378 100 bp using a linux one liner ( “awk ‘(\$3 >= 95)’ | awk ‘(\$4 >=100)’ | awk ‘{print \$1}’ | uniq >  
379 LIST”). We then extracted all these reads from the initial dataset using custom perl scripts (perl  
380 splitRNA.pl LIST). This subset of sequences was then blasted against all the previously extracted  
381 16S sequences from these SAGs (N = 4726 sequences), hits with a percent identity higher or  
382 equal to 98% over at least 100 bp were chosen selected as high quality chimeric reads ( “awk

383 '\$(3 >= 98)' | awk '\$(4 >=100)' | awk '{print \$1}' | uniq" as above). Only the top blast hit of the  
384 16S region is considered, while all the hits higher than 95% ID on the non-rRNA regions were  
385 considered equally good. This last constraint implies that if a read matches one 16S sequence  
386 and five non-16S SAG sequences it will appear counted in the matrix of figure 1b five times.  
387 We only validated using the 16S/18S gene.

388

389 *Identification of novel-virus host linkages.* The initial dataset (76M reads) was blasted  
390 against the final viral contig assembly from our previous work<sup>13</sup> (N = 99907 contigs, > 5Kb) with  
391 all default settings (Options= "blastn -outfmt 6 – num\_threads 8"). We then extracted a list of  
392 sequences that matched anything within that database using a Linux one liner ( "awk '{print \$1}'  
393 | uniq" ), at this point we did not filter for any level of identity. We then extracted all these  
394 reads from the initial dataset using custom perl scripts ("perl splitRNA.pl LIST"). This subset of  
395 sequences was then blasted against SILVA<sup>15</sup> and an in house collection of local near-full length  
396 16S-ITS clone sequences<sup>18</sup>. High quality chimeric reads were then identified using custom Perl  
397 scripts, and were chosen if between 40 and 60 percent of the read is covered by a match in one  
398 database and the rest by another match in the other database and if the minimum length of  
399 either alignment is 100 bp ("perl PartialAlignment.pl"). We found 1.5 M reads that were  
400 identified as high-quality chimeras linking contigs from the 5Yr virome and a ribosomal RNA  
401 molecule. Many of these hits were to cellular fragments within the 5Yr virome, so we curated  
402 further using different bioinformatic pipelines. We narrowed the final contig list to include only  
403 contigs that met one of the following criteria: VirSorter<sup>28</sup> (Categories 1 to 3), DeepVirFinder ( Scores  
404 > 0.9) were selected, MEGAN-LR<sup>29</sup>, CheckV<sup>30</sup> and by finding homologies to proteins  
405 within Tara viral proteomics datasets<sup>31</sup> (see below); The identification tool used for each contig  
406 is depicted in figure 2C, and all the values from each pipeline are in Suppl. Table 1. Each read  
407 was uniquely assigned to the contig as the top hit with the additional minimum identity to be  
408 95%. The other end of the reads was assigned to the top hit in the previously described clone  
409 database and to silva if the closest match within the local clones databases was lower than 95%  
410 and/or the chimeras was formed with 23S rRNA (Suppl. File 1).

411

412 *Additional curation of viral contigs.* Contigs were annotated using the top blastp hit to nr  
413 (Accessed August 2020). Additionally, we used the virus proteomic<sup>31</sup> dataset from Tara to  
414 inform some of the annotations of our dataset as viral, this second approach identified  
415 structural proteins in 33 contigs (Suppl. File Table 1). For MEGAN-LR, contigs were aligned using  
416 LAST<sup>32</sup> to the NCBI nt database (June 20, 2019) and the results were input to MEGAN-LR<sup>29</sup> using  
417 the lowest common ancestor (LCA) algorithm. CheckV was run using default settings using  
418 checkv-db-v0.6. Viral contigs were predicted de novo on contigs longer than 2000 bp using  
419 DeepVirFinder<sup>33</sup> requiring a p-value of 0.01.

420

421 *16S PCR amplification and ASV calling.* Prokaryotic DNA (0.2-1 um fraction)  
422 corresponding to the sampling dates overlapping with our metagenomic work was extracted as  
423 described by Chow et al.<sup>34</sup>. V4 and V5 regions were amplified using the primers described by  
424 Parada et al.<sup>35</sup>, following the methods described by Yeh et al<sup>36</sup>. ASVs used in this study have  
425 been deposited at <https://github.com/phagenomics/VirHostLinker>.

426

427       **Code Availability and Supplementary Information:** Custom code and supplementary  
428       files (for pre-print version) available at <https://github.com/phagenomics/VirHostLinker>.  
429       Formatted bash scripts to obtain the results presented in this manuscript can also be found  
430       there.  
431

432       **Data availability:** All data needed to evaluate the conclusions in the paper are present in  
433       the paper or the supplementary materials. Final cross-assembled sequences and raw  
434       sequencing data are deposited at NCBI under the BioProject PRJNA672948.  
435

436       **Author Contributions:** JCIE and JF conceived and designed the experiment; SL, YCY, SH,  
437       and AML contributed with bioinformatic pipelines, analyses, and databases. JW contributed  
438       with data visualization and statistical analyses. JCIE, SL, JW, YCY, SH, AML and JF contributed  
439       and commented on the final form of this manuscript.  
440

441       References:  
442

- 443       1. Breitbart, M., Bonnain, C., Malki, K. & Sawaya, N. A. Phage puppet masters of the marine  
444       microbial realm. *Nature Microbiology* (2018) doi:10.1038/s41564-018-0166-y.
- 445       2. Falkowski, P. G., Fenchel, T. & Delong, E. F. The microbial engines that drive earth's  
446       biogeochemical cycles. *Science* (2008) doi:10.1126/science.1153213.
- 447       3. Ahlgren, N. A., Ren, J., Lu, Y. Y., Fuhrman, J. A. & Sun, F. Alignment-free d2\*  
448       oligonucleotide frequency dissimilarity measure improves prediction of hosts from  
449       metagenomically-derived viral sequences. *Nucleic Acids Res.* (2017)  
450       doi:10.1093/nar/gkw1002.
- 451       4. Deng, L. *et al.* Viral tagging reveals discrete populations in *Synechococcus* viral genome  
452       sequence space. *Nature* (2014) doi:10.1038/nature13459.
- 453       5. Labonté, J. M. *et al.* Single-cell genomics-based analysis of virus-host interactions in  
454       marine surface bacterioplankton. *ISME J.* (2015) doi:10.1038/ismej.2015.48.
- 455       6. de Jonge, P. A. *et al.* Adsorption sequencing (AdsorpSeq) as a rapid method to link  
456       environmental bacteriophages to hosts. *iScience* (2020) doi:10.1016/j.isci.2020.101439.
- 457       7. Tadmor, A. D., Ottesen, E. A., Leadbetter, J. R. & Phillips, R. Probing individual  
458       environmental bacteria for viruses by using microfluidic digital PCR. *Science* (80-. ). (2011)  
459       doi:10.1126/science.1200758.
- 460       8. Bickhart, D. M. *et al.* Assignment of virus and antimicrobial resistance genes to microbial  
461       hosts in a complex microbial community by combined long-read assembly and proximity  
462       ligation. *Genome Biol.* (2019) doi:10.1186/s13059-019-1760-x.
- 463       9. Marbouth, M., Baudry, L., Cournac, A. & Koszul, R. Scaffolding bacterial genomes and  
464       probing host-virus interactions in gut microbiome by proximity ligation (chromosome  
465       capture) assay. *Sci. Adv.* (2017) doi:10.1126/sciadv.1602105.
- 466       10. Dekker, J., Rippe, K., Dekker, M. & Kleckner, N. Capturing chromosome conformation.  
467       *Science* (80-. ). (2002) doi:10.1126/science.1067799.
- 468       11. Sharma, E., Sterne-Weiler, T., O'Hanlon, D. & Blencowe, B. J. Global Mapping of Human  
469       RNA-RNA Interactions. *Mol. Cell* (2016) doi:10.1016/j.molcel.2016.04.030.
- 470       12. Trendel, J. *et al.* The Human RNA-Binding Proteome and Its Dynamics during

471 13. Translational Arrest. *Cell* (2019) doi:10.1016/j.cell.2018.11.004.

472 13. Ignacio-Espinoza, J. C., Ahlgren, N. A. & Fuhrman, J. A. Long-term stability and Red

473 Queen-like strain dynamics in marine viruses. *Nature Microbiology* (2019)

474 doi:10.1038/s41564-019-0628-x.

475 14. Roux, S. *et al.* Ecogenomics and potential biogeochemical impacts of globally abundant

476 ocean viruses. *Nature* (2016) doi:10.1038/nature19366.

477 15. Glöckner, F. O. *et al.* 25 years of serving the community with ribosomal RNA gene

478 reference databases and tools. *Journal of Biotechnology* (2017)

479 doi:10.1016/j.jbiotec.2017.06.1198.

480 16. Cram, J. A. *et al.* Seasonal and interannual variability of the marine bacterioplankton

481 community throughout the water column over ten years. *ISME J.* (2015)

482 doi:10.1038/ismej.2014.153.

483 17. Pachiadaki, M. G. *et al.* Charting the Complexity of the Marine Microbiome through

484 Single-Cell Genomics. *Cell* (2019) doi:10.1016/j.cell.2019.11.017.

485 18. Brown, M. V. & Fuhrman, J. A. Marine bacterial microdiversity as revealed by internal

486 transcribed spacer analysis. *Aquat. Microb. Ecol.* (2005) doi:10.3354/ame041015.

487 19. Hoarfstok, A. *et al.* Global ecotypes in the ubiquitous marine clade SAR86. *ISME J.* (2020)

488 doi:10.1038/s41396-019-0516-7.

489 20. Brum, J. R. *et al.* Patterns and ecological drivers of ocean viral communities. *Science* (80-)

490 J. (2015) doi:10.1126/science.1261498.

491 21. Ahlgren, N. A., Perelman, J. N., Yeh, Y. C. & Fuhrman, J. A. Multi-year dynamics of fine-

492 scale marine cyanobacterial populations are more strongly explained by phage

493 interactions than abiotic, bottom-up factors. *Environ. Microbiol.* (2019)

494 doi:10.1111/1462-2920.14687.

495 22. Sieradzki, E. T., Ignacio-Espinoza, J. C., Needham, D. M., Fichot, E. B. & Fuhrman, J. A.

496 Dynamic marine viral infections and major contribution to photosynthetic processes

497 shown by spatiotemporal picoplankton metatranscriptomes. *Nat. Commun.* **10**, 1169

498 (2019).

499 23. Martinez-Hernandez, F. *et al.* Single-cell genomics uncover Pelagibacter as the putative

500 host of the extremely abundant uncultured 37-F6 viral population in the ocean. *ISME J.*

501 (2019) doi:10.1038/s41396-018-0278-7.

502 24. Warwick-Dugdale, J. *et al.* Long-read viral metagenomics captures abundant and

503 microdiverse viral populations and their niche-defining genomic islands. *PeerJ* (2019)

504 doi:10.7717/peerj.6800.

505 25. Boyd, J. A., Woodcroft, B. J. & Tyson, G. W. GraftM: a tool for scalable, phylogenetically

506 informed classification of genes within metagenomes. *Nucleic Acids Res.* (2018)

507 doi:10.1093/nar/gky174.

508 26. Chen, S., Zhou, Y., Chen, Y. & Gu, J. Fastp: An ultra-fast all-in-one FASTQ preprocessor. in

509 *Bioinformatics* (2018). doi:10.1093/bioinformatics/bty560.

510 27. Aronesty, E. ea-utils : Command-line tools for processing biological sequencing data.

511 *Expr. Anal. Durham* (2011) doi:<http://code.google.com/p/ea-utils>.

512 28. Roux, S., Enault, F., Hurwitz, B. L. & Sullivan, M. B. VirSorter: mining viral signal from

513 microbial genomic data. *PeerJ* (2015) doi:10.7717/peerj.985.

514 29. Huson, D. H. *et al.* MEGAN-LR: New algorithms allow accurate binning and easy

515 interactive exploration of metagenomic long reads and contigs. *Biol. Direct* (2018)  
516 doi:10.1186/s13062-018-0208-7.

517 30. Nayfach, S., Pedro Camargo, A., Eloé-Fadros, E. & Roux, S. CheckV: assessing the quality  
518 of metagenome-assembled viral genomes. *bioRxiv* (2020)  
519 doi:10.1101/2020.05.06.081778.

520 31. Brum, J. R. *et al.* Illuminating structural proteins in viral ‘dark matter’ with  
521 metaproteomics. *Proc. Natl. Acad. Sci. U. S. A.* (2016) doi:10.1073/pnas.1525139113.

522 32. Kiełbasa, S. M., Wan, R., Sato, K., Horton, P. & Frith, M. C. Adaptive seeds tame genomic  
523 sequence comparison. *Genome Res.* (2011) doi:10.1101/gr.113985.110.

524 33. Ren, J. *et al.* Identifying viruses from metagenomic data using deep learning. *Quant. Biol.*  
525 (2020) doi:10.1007/s40484-019-0187-4.

526 34. Chow, C. E. T. *et al.* Temporal variability and coherence of euphotic zone bacterial  
527 communities over a decade in the Southern California Bight. *ISME J.* (2013)  
528 doi:10.1038/ismej.2013.122.

529 35. Parada, A. E., Needham, D. M. & Fuhrman, J. A. Every base matters: Assessing small  
530 subunit rRNA primers for marine microbiomes with mock communities, time series and  
531 global field samples. *Environ. Microbiol.* (2016) doi:10.1111/1462-2920.13023.

532 36. Yeh, Y.-C., McNichol, J. C., Needham, D. M., Fichot, E. B. & Fuhrman, J. A. Comprehensive  
533 single-PCR 16S and 18S rRNA community analysis validated with mock communities and  
534 denoising algorithms. *bioRxiv* 866731 (2019) doi:10.1101/866731.

535

536